



LAWRENCE
LIVERMORE
NATIONAL
LABORATORY

AMR Code Simulations of Turbulent Combustion in Confined and Unconfined SDF Explosions

Allen L. Kuhl, John B. Bell, Vincent Beckner

June 5, 2009

HPCMP Users Group Meeting
San Diego, CA, United States
June 15, 2009 through June 19, 2009

Disclaimer

This document was prepared as an account of work sponsored by an agency of the United States government. Neither the United States government nor Lawrence Livermore National Security, LLC, nor any of their employees makes any warranty, expressed or implied, or assumes any legal liability or responsibility for the accuracy, completeness, or usefulness of any information, apparatus, product, or process disclosed, or represents that its use would not infringe privately owned rights. Reference herein to any specific commercial product, process, or service by trade name, trademark, manufacturer, or otherwise does not necessarily constitute or imply its endorsement, recommendation, or favoring by the United States government or Lawrence Livermore National Security, LLC. The views and opinions of authors expressed herein do not necessarily state or reflect those of the United States government or Lawrence Livermore National Security, LLC, and shall not be used for advertising or product endorsement purposes.

AMR Code Simulations of Turbulent Combustion in Confined and Unconfined SDF Explosions[‡]

Allen L. Kuhl¹, John B. Bell² & Vincent E. Beckner²

¹Lawrence Livermore National Laboratory
7000 East Avenue, Livermore, California, USA 94551

²Lawrence Berkeley National Laboratory
1 Cyclotron Road, Berkeley, California, USA 94551

Abstract

A heterogeneous continuum model is proposed to describe the dispersion and combustion of an aluminum particle cloud in an explosion. It combines the gas-dynamic conservation laws for the gas phase with a continuum model for the dispersed phase, as formulated by Nigmatulin. Inter-phase mass, momentum and energy exchange are prescribed by phenomenological models. It incorporates a combustion model based on the mass conservation laws for fuel, air and products; source/sink terms are treated in the fast-chemistry limit appropriate for such gasdynamic fields, along with a model for mass transfer from the particle phase to the gas. The model takes into account both the afterburning of the detonation products of the booster with air, and the combustion of the Al particles with air. The model equations were integrated by high-order Godunov schemes for both the gas and particle phases. Numerical simulations of the explosion fields from 1.5-g Shock-Dispersed-Fuel (SDF) charge in a 6.6 liter calorimeter were used to validate the combustion model. Then the model was applied to 10-kg Al-SDF explosions in a vented two-room structure and in an unconfined height-of-burst explosion. Computed pressure histories are in reasonable (but not perfect) agreement with measured waveforms. Differences are caused by physical-chemical kinetic effects of particle combustion which induce ignition delays in the initial reactive blast wave and quenching of reactions at late times. Current simulations give initial insights into such modeling issues.

1. Introduction

Laboratory experiments have been performed with 1.5-gram Shock-Dispersed-Fuel (SDF) charges [1]. The charge consisted of a 0.5-g PETN booster surrounded by 1-g of flake Aluminum (Al) powder. The SDF charge was placed at the center of a bomb calorimeter. Detonation of the booster disperses the fuel, ignites it, and induces an exothermic energy release via a turbulent combustion process. Over-pressure histories in air were considerably larger than those measured in nitrogen atmospheres; impulses histories show factors of 2 to 4 increase due to Al-air combustion. At the 2007 HPCMP Users Group Meeting, we reported on numerical simulations of those experiments that were performed with our two-phase 3D AMR code [2].

Here we study the flow fields created by confined and un-confined SDF explosions at the 10-kg scale. In particular, we consider an SDF charge consisting of 3.6-kg spherical C4 booster surrounded by 6.4-kg of flake Al powder. The charge was detonated 122 cm above a concrete pad instrumented with static pressure gages. Described here are numerical simulations of the explosion field performed with our three-dimensional (3D) adaptive mesh refinement (AMR) code. The

combustion model treats the flow field as a dilute heterogeneous continuum—with separate conservation laws for each phase—and interaction terms that allow the phases to exchange mass, momentum and energy via phenomenological laws [3]. A unique feature of the model is that a high-order Godunov algorithm is used not only for the gas phase, but also for the particle phase. This provides an accurate solution of the governing hyperbolic conservation laws that is devoid of artificial effects of numerical diffusion. The system of equations is closed by a quadratic EOS model that specifies the thermodynamic states of the combustion fields. Results of the AMR code simulations of the 10 kg-SDF explosions will be described and compared with experimental results.

2. Model

2.1 Conservation Laws

The Model is based on the Eulerian multi-phase conservation laws for a dilute heterogeneous continuum [3,4]. We model the evolution of the gas phase combustion fields in the limit of large Reynolds and Peclet numbers, where effects of molecular diffusion and heat conduction are negligible. The flow field is governed by the gas-dynamic conservation laws:

$$\text{Mass:} \quad \partial_t \rho + \nabla \cdot (\rho \mathbf{u}) = \dot{\sigma}_s \quad (1)$$

$$\text{Momentum:} \quad \partial_t \rho \mathbf{u} + \nabla \cdot (\rho \mathbf{u} \mathbf{u} + p) = \dot{\sigma}_s \mathbf{v} - \dot{f}_s \quad (2)$$

$$\text{Energy:} \quad \partial_t \rho E + \nabla \cdot (\rho \mathbf{u} E + p \mathbf{u}) = -\dot{q}_s + \dot{\sigma}_s E_s - \dot{f}_s \cdot \mathbf{v} \quad (3)$$

where ρ, p, u represent the gas density, pressure and specific internal energy, \mathbf{u} is the gas velocity vector, and $E \equiv u + \mathbf{u} \cdot \mathbf{u}/2$ denotes the total energy of the gas phase. Source terms on the right hand side take into account: mass addition to gas phase due to particle burning ($\dot{\sigma}_s$), particle drag (\dot{f}_s), and heat losses (\dot{q}_s).

We treat the particle phase as a Eulerian continuum field [3,4]. We consider the dilute limit, devoid of particle-particle interactions, so that the pressure and sound speed of the particle phase are zero. We model the evolution of particle phase mass, momentum and energy fields by the conservation laws of continuum mechanics for heterogeneous media:

$$\text{Mass:} \quad \partial_t \sigma + \nabla \cdot \sigma \mathbf{v} = -\dot{\sigma}_s \quad (4)$$

$$\text{Momentum:} \quad \partial_t \sigma \mathbf{v} + \nabla \cdot \sigma \mathbf{v} \mathbf{v} = -\dot{\sigma}_s \mathbf{v} + \dot{f}_s \quad (5)$$

$$\text{Energy:} \quad \partial_t \sigma E_s + \nabla \cdot \sigma E_s \mathbf{v} = \dot{q}_s - \dot{\sigma}_s E_s + \dot{f}_s \cdot \mathbf{v} \quad (6)$$

where σ and \mathbf{v} represent the particle-phase density and velocity and $E_s \equiv C_s T_s$ denotes the energy of the particle phase.

2.2 Interactions

The inter-phase interaction terms for mass, momentum, and heat take the form as described by Khasainov et al. (2005):

$$\text{Mass Exchange:} \quad \dot{\sigma}_s = \begin{cases} 0 & T_s < T_{melt} \\ -3\sigma(1 + 0.276\sqrt{\text{Re}_s})/t_s & T_s \geq T_{melt} \end{cases} \quad (7)$$

$$\text{Momentum Exchange:} \quad \dot{f}_s = (3\rho\sigma/4\rho_s d_s) C_D (\mathbf{u} - \mathbf{v}) |\mathbf{u} - \mathbf{v}| \quad (8)$$

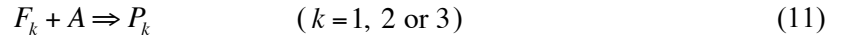
$$\text{Heat Exchange:} \quad \dot{q}_s = (6\sigma/\rho_s d_s) \left[\text{Nu} \lambda (T - T_s) / d_s + \varepsilon \sigma_{\text{Boltz}} (T^4 - T_s^4) \right] \quad (9)$$

$$\text{Burning Law:} \quad t_s = K d_{s0}^2 \quad (10)$$

where $C_D = 24/\text{Re}_s + 4.4/\sqrt{\text{Re}_s} + 0.42$ and $\text{Re}_s = \rho d_s |\mathbf{u} - \mathbf{v}|/\mu$ and $Nu = 2 + 0.6 \text{Pr} \sqrt{\text{Re}_s}$. Here, we assume the mass transfer from particles to continuum occurs at the melting point of Al and we view the Al in the continuum phase as a micro-mist of Al droplets in velocity and thermal equilibrium with the gas but does not contribute to pressure. An additional phase change is included at the vaporization temperature of Al, at which point it becomes a gas and contributes to the gas pressure.

2.3 Combustion

We consider three fuels: *C4* detonation products (F_1), Aluminum (F_2), and gaseous hydrocarbon (F_3), along with their corresponding combustion products: *C4*-air (P_1) and Al-air (P_2) and *CH*-air (P_3). (Al is assumed to only burn in the continuum phase). We consider global combustion of fuel F_k with air (A) producing equilibrium combustion products P_k :



The mass fractions Y_k of the components are governed by the following conservation laws:

$$\text{Fuel-}k: \quad \partial_t \rho Y_{F_k} + \nabla \cdot \rho Y_{F_k} \mathbf{u} = -\dot{s}_k + \delta_{k2} \dot{\sigma}_k \quad (12)$$

$$\text{Air:} \quad \partial_t \rho Y_A + \nabla \cdot \rho Y_A \mathbf{u} = -\sum_k \alpha_k \dot{s}_k \quad (13)$$

$$\text{Products-}k: \quad \partial_t \rho Y_{P_k} + \nabla \cdot \rho Y_{P_k} \mathbf{u} = \sum_k (1 + \alpha_k) \dot{s}_k \quad (14)$$

Fuel and air are consumed in stoichiometric proportions: $\alpha_k = A/F_k$. In the above, \dot{s}_k represents the global kinetics sink term. In this work we use the fast-chemistry limit that is consistent with the inviscid gas-dynamic model (1)-(3), so whenever fuel and air enter a computational cell, they are consumed in one time step. Here δ_{k2} represents the Kronecker delta ($\delta_{k2} = 0$ if $k \neq 2$ and $\delta_{k2} = 1$ if $k = 2$) and takes into account the mass transfer of Al from the particle phase EQ. (4) to the gas phase.

2.4 Equations of State

The thermodynamic states encountered during SDF explosions have been analyzed in by Kuhl and Khasainov [5]. The loci of states of component c in the specific internal energy-temperature ($u-T$) plane are fit with quadratic functions of temperature:

$$u_c(T) = a_c T^2 + b_c T + c_c \quad (15)$$

For cells containing a mixture of components, the mixture energy also satisfies a quadratic form:

$$u_m(T) = \sum_c Y_c u_c = a_m T_m^2 + b_m T_m + c_m \quad (16)$$

Given the mixture specific internal energy u_m , the mixture temperature can be evaluated by:

$$T_m = [-b_m + \sqrt{b_m^2 - 4a_m(c_m - u_m)}] / 2a_m \quad (17)$$

using mixture coefficients as defined by:

$$a_m = \sum_c Y_c a_c, \quad b_m = \sum_c Y_c b_c, \quad c_m = \sum_c Y_c c_c, \quad R_m = \sum_c Y_c R_c \quad (18)$$

For pure cells, the pressure of a component is calculated from the perfect gas relation $p_c = \rho_c R_c T_c$, or from the JWL function in the detonation products gases [4]. In mixed cells, the pressure is calculated from the mixture temperature by the ‘‘law of additive pressures’’:

$$p_m = \sum_c p_c(V_m, T_m) \quad (19)$$

where $p_c(V_m, T_m)$ denotes the pressure of component c if it existed alone at V_m and T_m .

2.5 Numerical Methods

The governing equations (1)-(6) and (12)-(14) are integrated with high-resolution upwind methods that represent high-order generalizations of Godunov's method. The algorithm for gas phase conservation laws is based on an efficient Riemann solver for gas-dynamics first developed by Colella and Glaz [6]. The algorithm for the particle phase conservation laws is based on a Riemann solver for two-phase flows developed by Collins et al. [7]. Source terms are treated with operator splitting methods. Being based on Riemann solvers, information propagates along characteristics at the correct wave speeds, and they incorporate nonlinear wave interactions within the cell during the time step.

These Godunov schemes have been incorporated into the embedded boundary adaptive mesh refinement (AMR) algorithm of Pember et al. [8] that allows us to focus computational effort in complex regions of the flow such as mixing layers and reaction zones. In this AMR approach, regions to be refined are organized into rectangular patches, with 100's to 1,000's of grid-points per patch. AMR is also used to refine turbulent mixing regions; by successive refinements we are able to capture the energy-bearing scales of the turbulence on the computational grid. In this way we are able to compute the effects of turbulent mixing without resorting to turbulence modeling (which is not applicable to this problem). This is consistent with the "MILES" approach of Boris et al. [9].

3. Results

We used the 3D two-phase AMR code to simulate the explosion of a 1.5-g Al-SDF charge (0.5-g PETN booster + 1-g flake Al) and the ensuing turbulent combustion with air in calorimeter A (right circular cylinder: $D=20$ cm, $L=21$ cm and $V=6.6$ liters). Computed pressure histories at $R=5$ cm on the lid of the vessel are compared with pressure measurements in Fig. 1. The computed waveform (black curve) is similar to the experiment in air (red curve). Both curves are considerably larger than the experimental data for the Al-SDF explosion in nitrogen (blue curve). Such comparisons illustrate the dramatic effect that combustion has on chamber pressures for SDF explosions. Evolution of the computed component masses (Al, PETN, air, Al-air products, PETN-air products) in calorimeter A are presented in Fig. 2. By 3 ms, more than 95% of the Al fuel and 90% of the PETN detonation products have been consumed by combustion.

Next, we performed 3D simulations of a 10-kg Al-SDF explosion in a vented two-room structure. The charge consisted of a 3.3-kg spherical C-4 booster surrounded by 6.7-kg of flake Al. Room dimensions are: $X=457$ cm by $Y=366$ cm in plan-form by $Z=244$ cm in height, with a volume of 40.8 m³. The charge was detonated in the center of room 1 at mid-height ($z=122$ cm). The fuel loading (i.e., chamber volume/fuel mass) was similar to the fuel loading of calorimeter A: 4.4 liters/g. Visualization of the temperature field at different times during the simulation is presented in Plate 1 (plan view cross-section at mid-height $z=122$ cm). Explosion of the booster accelerates the Al fuel into a thin shell just behind the shock (Frame 1). Temperatures are high enough to ignite the Al particles (red denotes 4,300 K). Shock reflections from the walls, floor and ceiling breakup the fuel shell (Frames 2 and 3), leading to intense turbulent combustion which fills the first room by 2.7 ms (Frame 4). A variety of mixing scales are evident.

Figure 3 depicts the pressure histories at ground zero (on the ceiling directly above the charge) for the 10-kg Al-SDF explosion in the two-room structure. The computed waveform (black curve) is narrower and has a higher peak than the measured waveform (red curve). Perhaps the numerical simulation burns faster and is less dissipative than the experiment; also, the measurement system used an eighth-order Bessel filter, which will broaden the waveform and lower its peak. Nevertheless, both waveforms are much larger than the waveform for the C-4 booster charge (blue curve)—thereby demonstrating that a reactive blast wave is formed during the initial charge expansion (Fig. 3a). At later times, the computed and measured waveforms are quite similar (Fig. 3b).

Next, 3D simulations of an unconfined 10-kg Al-SDF explosion at a height of burst (HOB) of 122 cm were performed. A cross-sectional view of the computed temperature field at 30 ms is

presented in Plate 2. Red corresponds to a temperature of 4,300 K, and illustrates where Al-air combustion is occurring within the explosion cloud. A variety of mixing scales are evident.

4. Conclusions

A heterogeneous continuum model of Al particle combustion in explosions is proposed. It is based on the underlying assumption that the combustion rate is limited by rate that fuel (Al and/or booster detonation products gases) are brought together with air by turbulent mixing. This represents the *fast-chemistry limit* for such reacting flows. We have shown this to be valid for gas phase combustion in explosions (e.g., afterburning of TNT detonation products with air). However, particle combustion introduces new characteristic scales (particle diameter, particle size distribution, surface coating, etc.) that can induce ignition delays due to physical-chemical kinetic effects not found in gaseous systems. Such kinetic effects could be important in the ignition of the reactive blast wave at early times, and in quenching of the reactions by mixing with air at late times. We plan to explore the importance of kinetic-effects modeling by performing simulations Al-SDF combustion in explosions at the 1.5-g scale (six different chamber experiments) and at the 10-kg scale (confined and unconfined field tests). Results shown here give initial insights into this process.

References

- [1] A. L. Kuhl, H. Reichenbach (2008) Combustion effects in confined explosions, *Proceedings of the Combustion Institute* **32** (2009) pp 2291-2298.
- [2] Bell, J. B., Beckner, V. E. & Kuhl, A. L. (2007) Simulation of enhanced explosive devices in chambers and tunnels (plenary lecture), *DOD High Performance Computing Users Group Conference 2007 (HPCMP-UGC 2007) 0-7695-3088-5/07 IEEE*, 5 pages.
- [3] A. L. Kuhl, J. B. Bell and V. E. Beckner (2009) Heterogeneous continuum model of Aluminum particle combustion in explosions, *Fizika Goreniya i Vzryva* (in press).
- [4] R. I. Nigmatulin (1987) *Dynamics of Multi-Phase Flows*. Vol. 1. Moscow, Nauka, 464 pp
- [5] A. L. Kuhl & B. Khasainov (2007) Quadratic model of thermodynamic states in SDF explosions, *Energetic Materials: 38th Int. Conf. ICT*, pp. 143.1-143.11.
- [6] P. Colella & H. Glaz (1985) Efficient solution algorithms for the Riemann problem for real gases", *J Comp. Phys.*, 59, pp. 264-289.
- [7] P. Collins, R. E. Ferguson, K. Chien, A. L. Kuhl, J. Krispin & H. M. Glaz (1994) Simulation of shock-induced dusty gas flows using various models, AIAA 94-2309.
- [8] R.B. Pember, J.B. Bell, P. Colella, W.Y. Crutchfield, and M.L. Welcome, "An Adaptive Cartesian Grid Method for Unsteady Compressible Flow in Irregular Regions," *J. Comp. Phys.*, 120:2, pp. 278-304, 1995.
- [9] J. Boris et al (1992) "New insights into large eddy simulation". *Fluid Dynamics Research*, 10.

ACKNOWLEDGEMENTS

This work performed under the auspices of the U.S. Department of Energy by Lawrence Livermore National Laboratory under Contract DE-AC52-07NA27344. The work at LBNL was performed under U.S. Department of Energy under Contract No. DE-AC02-05CH11231. This work was sponsored by the Defense Threat Reduction Agency under IACRO's 08-43991 and 09-45091; Dr. William Wilson, DTRA/CXWJ, is the contract monitor; his support is greatly appreciated.

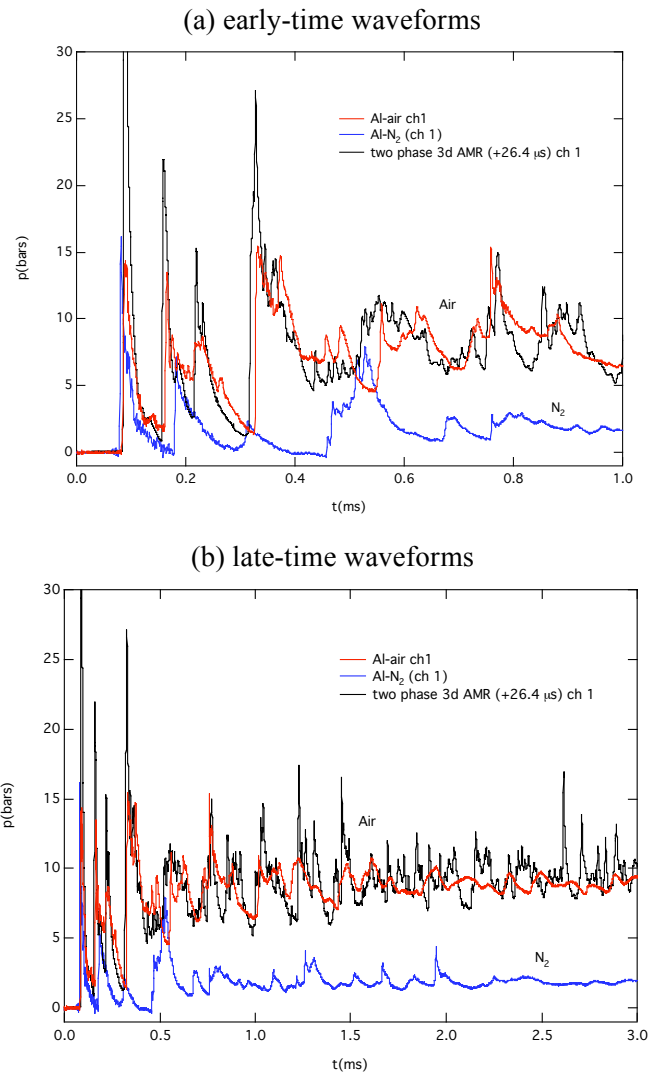


Figure 1. Pressure histories corresponding to 1.5-g Al-SDF charge explosion in calorimeter A.

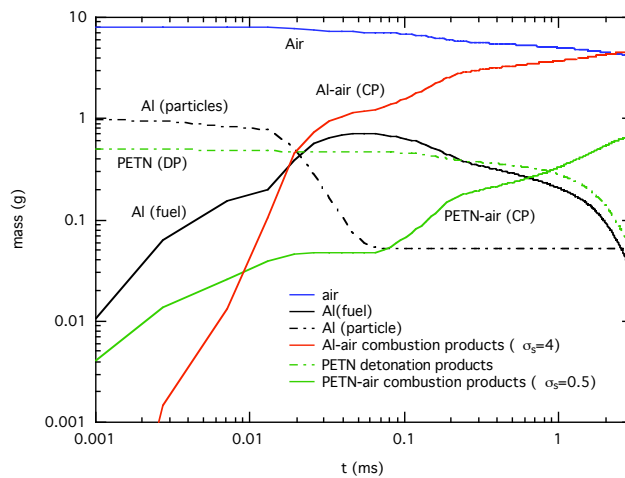


Figure 2. Computed evolution of component masses from combustion in calorimeter A.

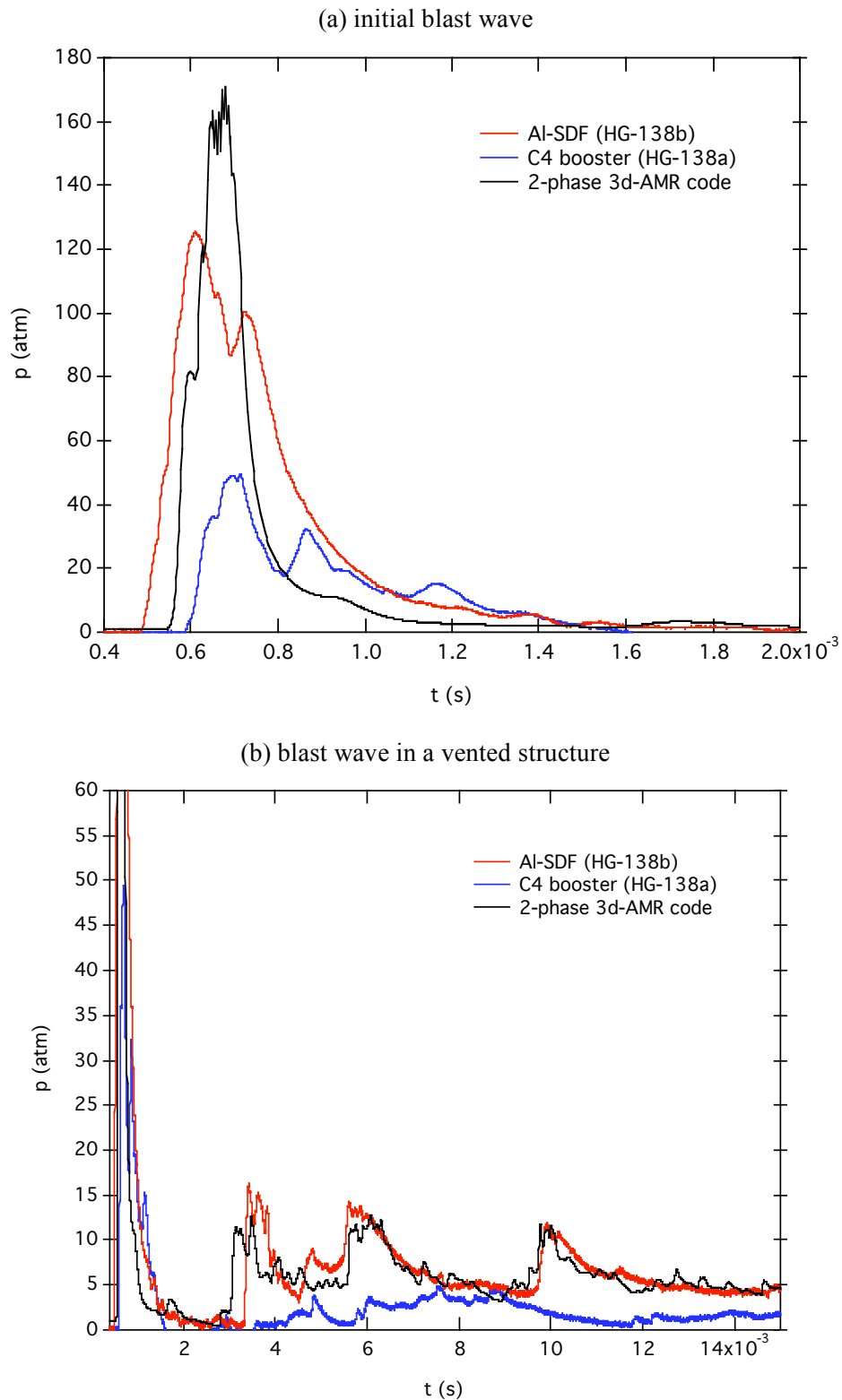


Figure 3. Blast wave pressure histories measured at ground zero (below the charge) for the SDF charge (red curve) versus the booster charge (blue curve) illustrating the reactive blast wave effect. Black curve represents the 3D simulation with the two-phase AMR code.

COLOR PLATE

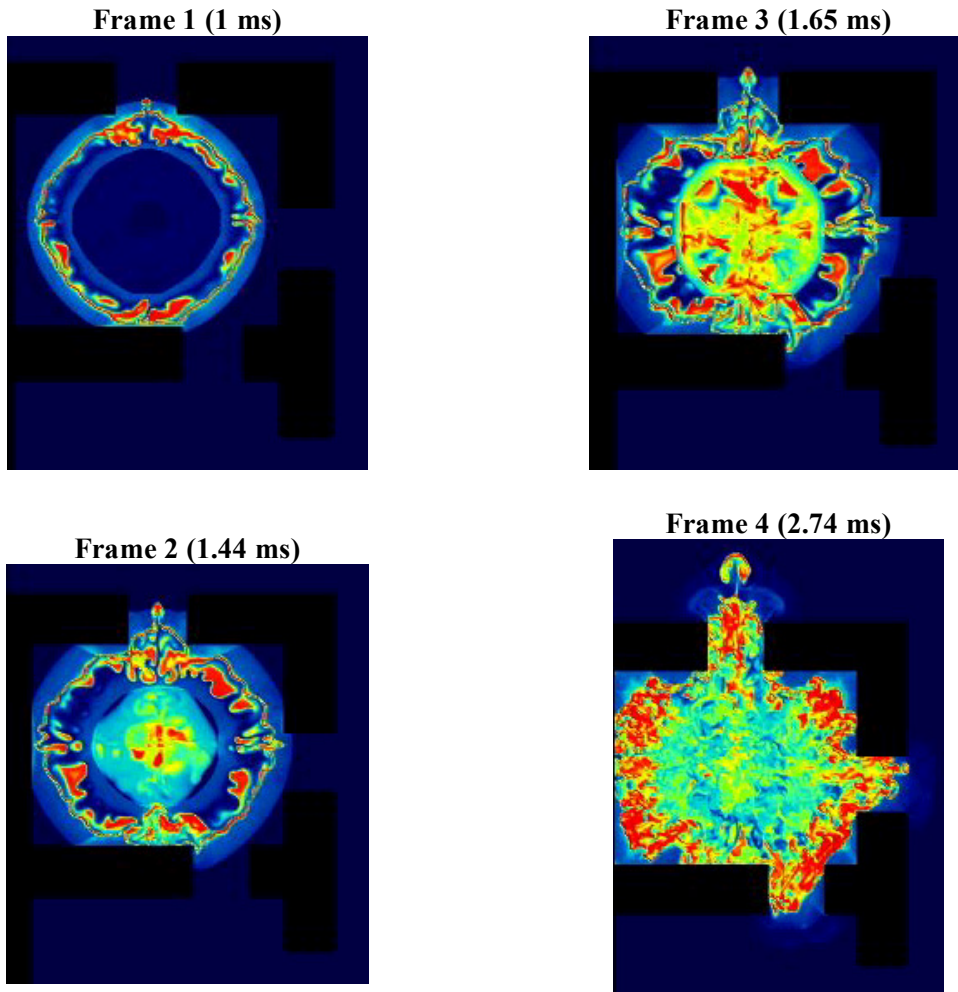


Plate 1. Visualization of the temperature field from a 10-kg Al-SDF explosion in a vented two-room structure; this represents plan view cross-section of the flow at mid-height ($z = 122$ cm).

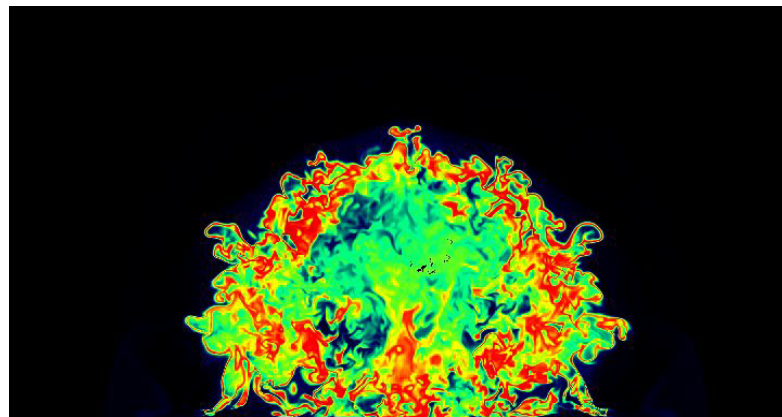


Plate 2. Temperature field illustrating Al-air combustion in an unconfined 10-kg SDF explosion cloud (HOB=122 cm, $t = 30$ ms).